Parasitol Res (2004) 92: 317–327
DOI 10.1007/s00436-003-1057-5

ORIGINAL PAPER

Steven P. O'Hara · Jae-Ran Yu · Jim Jung-Ching Lin

A novel *Cryptosporidium parvum* antigen, CP2, preferentially associates with membranous structures

Received: 7 July 2003 / Revised: 24 November 2003 / Accepted: 24 November 2003 / Published online: 16 January 2004

Abstract The present study addresses the cloning and characterization of a *Cryptosporidium parvum* antigen, CP2. Sequencing of cDNA and genomic clones revealed a novel gene capable of coding a message of 2,136 nucleotides flanked by 28 and 140 nucleotides of the 5′- and 3′-noncoding regions, respectively. The deduced amino acid sequence suggests that CP2 is a secreted and/or membrane protein. Immunofluorescence microscopy detected CP2 enrichment in sporozoites that subsequently appeared to encase type I meronts in infected HCT-8 cells. Immunogold electron microscopy revealed that CP2 consistently localized to membranous structures throughout development. In addition, progression from macrogametocyte to sporulated oocyst revealed CP2 initially at the periphery of amylopectin-like granules, in the cytoplasm and discrete vesicles, the parasitophorous vacuole, on the surface of sporozoites, and finally on the parasitophorous vacuole membrane (PVM). The observed expression pattern suggests that CP2 may be involved in the invasion process and/or PVM integrity.

Introduction

Cryptosporidiosis is now recognized as a worldwide health risk to humans, especially those individuals with compromised immune systems. Interestingly, drugs found to be effective against other apicomplexans are ineffective against human cryptosporidiosis. In fact, there is no consistently effective treatment for cryptosporidiosis. A greater understanding of the infection process and the niche occupied by *Cryptosporidium parvum* within host enterocytes may aid in the discovery of novel treatment avenues.

During infection, *C. parvum* occupies a unique niche on the brush border of enterocytes. The outer envelope and parasitophorous vacuole membrane (PVM) are derived from host membrane that rises up and engulfs the infective zoite (Tzipori and Griffiths 1998). The parasitophorous vacuole separates the outer parasite pellicle membrane from the host-derived PVM with the exception of the region of membrane fusion at the annular ring (Lumb et al. 1988). Previous studies utilizing monoclonal antibodies localized some *Cryptosporidium* antigens to the host-derived PVM (Bonnin et al. 1995; McDonald et al. 1995; Robert et al. 1994), suggesting that the PVM is modified by parasite proteins. However, the molecular nature of these modifications is not known. In addition, these monoclonal antibodies were shown to react to carbohydrate epitopes. Thus, the usage of these antibodies is limited.

Apicomplexans rely on secreted molecules present in highly differentiated apical complex organelles for host cell selection, invasion, and intracellular survival (Carruthers and Sibley 1997; Dubremetz et al. 1998). Similarly, modification of host-derived membranes by the parasite may also be important for these processes during the maturation process. In the present study, we cloned a novel gene, *cp2*, from *C. parvum*, whose gene product may be a secreted and/or membrane protein. Using immunofluorescence and immunoelectron microscopy, it was determined that the CP2 protein is found on sporozoites and consistently, yet minimally, localizes to the PVM of trophozoites and type I meronts. During sexual development of the parasite, the CP2 protein was found to be more highly expressed. It was initially located in amylopectin-like granules and the cytoplasm of macrogametocytes and subsequently on the PVM, oocyst wall, and sporozoites of developing and sporulated oocysts.

S. P. O'Hara · J. J.-C. Lin (✉)
Department of Biological Sciences, University of Iowa,
138 Biology Building, Iowa City, IA 52242-1324, USA
E-mail: jim-lin@uiowa.edu
Tel.: +1-319-3351075
Fax: +1-319-3351069

J.-R. Yu
Department of Parasitology, College of Medicine,
Konkuk University, 380-701 Chungju, Korea

Materials and methods

Isolation of CP2 cDNA and genomic DNA clones

Both the Iowa isolate *C. parvum* cDNA expression library and genomic DNA library were obtained from the National Institutes of Health AIDS Reagent and Reference Program. The λZAPII *C. parvum* cDNA library was initially screened using a mouse monoclonal antibody (mAb), CMYL30, specific for the oocyst wall antigen CM250 (Yu et al. 2002), as described by Jin and Lin (1989). A clone, SC1, was obtained. While further studies suggested that SC1 was not recognized by the CMYL mAb, sequence characteristics prompted further investigation. A 600-bp cDNA insert from SC1 was radioactively labeled with the Random primed DNA labeling kit (Boehringer Mannheim) and used as a probe to screen the same λZAPII library. The hybridization reaction was carried out at 55 °C for 2 h in Quikhyb solution (Stratagene, La Jolla, Calif.) containing 100 μg salmon sperm DNA/ml and 1×10^6 cpm labeled probe/ml. The membranes were washed briefly with 2× SSC, 0.1% SDS at room temperature followed by two washes (15 min each) with 0.1× SSC, 0.1%SDS at 37 °C. The membranes were exposed to film at −70 °C with intensifier screens. Numerous positive plaques were obtained and plaque-purified. Plasmids from positive plaques were zapped-out by in vivo excision, using the Ex-Assist helper phage as described by the manufacturer. Sequencing of the inserts was performed at the DNA Core Facility, University of Iowa, Iowa City, Iowa. The λZAPII genomic DNA library was screened using the same protocol. Five positive plaques were plaque-purified and inserts were sequenced as above.

Expression of a CP2 glutathione-S-transferase fusion protein and production of antibody against CP2

The 600 bp insert from SC1 was subcloned into a pGEX-4T3 vector in the same reading frame of glutathione-*S*-transferase (GST). After sequence verification, the recombinant GST-CP2 fusion protein was first expressed in *Escherichia coli* BL21(DE3)pLysS cells and purified by glutathione Sepharose 4B beads, according to the instructions provided by the manufacturer (Pharmacia, Piscataway, N.J.). The GST-CP2 was then used to immunize White New Zealand female rabbits. The antibodies obtained and pre-immune serum were analyzed by ELISA and Western blot.

Oocyst purification and cell culture infection

Oocysts of *C. parvum* were obtained from the feces of C57BL female mice (orally infected with 2×10^6 oocysts/mouse at 3 weeks of age) with a slight modification (Yu et al. 2002) of a previously described method (Yu 1998). Mouse feces were examined by modified Ziehl–Neelsen staining to confirm oocyst shedding (Casemore et al. 1985), collected in 2.5% potassium dichromate, and stored at 4 °C. The oocysts were purified as described by Petry et al. (1995). Cell culture infections were performed as described by Upton et al. (1995). Briefly, human ileocecal adenocarcinoma (HCT-8) cells were maintained in RPMI 1640 media with 5% horse serum. Prior to oocyst inoculation, HCT-8 cells were plated onto coverslips and grown in RPMI 1640 with 10% bovine serum albumin (BSA) supplemented with Hepes, glucose, ascorbic acid, folic acid, 4-aminobenzoic acid, calcium pantothenate, insulin, penicillin, streptomycin, and amphotericin B (Fungizone; supplemental media). Purified oocysts were treated with ice-cold 10% Clorox bleach, washed twice in ice-cold sterile water, resuspended in supplemental media, and added to culture dishes at a concentration of $2–5\times10^5$ oocysts/dish (60 mm diameter). Infections were allowed to proceed for 10–24 h.

Immunogold labeling

The small intestine of *C. parvum*-infected mice were dissected out at 14 days post-infection and fixed in 2% paraformaldehyde, 0.4% glutaraldehyde for approximately 2 h at room temperature. Fixed tissues were washed with 0.1 *M* phosphate buffer (pH 7.2) and dehydrated through a 30–95% graded alcohol series. Dehydrated tissues were embedded in LR gold resin (London Resin Co., London, UK) and polymerized at −20 °C for 72 h under UV illumination. Ultrathin sectioning was performed at a thickness of 90 nm and sections were mounted onto nickel grids. The immunogold labeling procedure followed the methods of Yu and Chai (1995). Briefly, tissue sections were incubated in PBS-milk-Tween (PMT: 3% skim milk, 0.01% Tween 20 in PBS) for 10 min and exposed to rabbit anti-CP2 antiserum diluted with PMT for 2 h at room temperature. The sections were washed thoroughly with PBS-BSA-Tween (1% BSA, 0.01% Tween 20 in PBS) and incubated overnight with 5-nm gold-conjugated goat anti-rabbit IgG (Sigma Chemical Co., St. Louis, Mo.) at 4 °C. Silver enhancement was performed with a commercial kit (Amersham Life Science, UK) followed by staining with uranyl acetate and lead citrate. The stained sections were examined under a transmission electron microscope (Jeol 1200 EXII).

Immunohistochemical staining

The small intestine of *C. parvum*-infected mice were dissected out at 14 days post-infection and fixed overnight in 3.7% formaldehyde, dehydrated, cleared in xylene, and embedded in Paraplast Plus (Oxford, St. Louis, Mo.). The small intestine of control mice were also dissected out and fixed as above. Serial sections (7 μm) were mounted on glass slides, rinsed in xylene, and rehydrated. Following pre-treatment with 0.3% hydrogen peroxide for 30 min and 10% donkey serum for 20 min, sections were incubated with the anti-CP2 polyclonal antibody for 30 min at room temperature, followed by several washings in PBS (5 min each). Sections were subsequently incubated in a 1:1,000 dilution of biotin-SP-conjugated donkey anti-rabbit IgG for 45 min, washed for 5 min in PBS, and treated with a 1:400 dilution of peroxidase-conjugated streptavidin for 15 min at room temperature. Sections were again washed in PBS before incubation with diaminobenzidine according to the manufacturer's instructions (Vector Laboratories, Burlingame, Calif.).

Immunofluorescence microscopy

Infected cells grown on coverslips were removed from dishes after appropriate incubation times, immediately washed in PBS, fixed for 5 min in 3.7% formaldehyde, and rinsed again in PBS. The cells were permeabilized with 0.01% Triton X-100 for 3 min and rinsed again in PBS. The rabbit anti-CP2 antiserum and control rabbit pre-immune serum were diluted 1:100 in Dulbecco′s modified Eagle′s medium supplemented with 5% BSA. Coverslips were incubated in primary antibody at 37 °C in a humidified chamber for 30 min and then rinsed in PBS, followed by a 1:300 dilution of rhodamine-conjugated goat anti-rabbit IgG whole-molecule antibody (Cappel, West Chester, Pa.) in PBS for 30 min. All coverslips were then treated with 0.2% 4′,6-diamidino-2-phenylindole in PBS for 15 min, washed, mounted in gelvatol (Hegmann et al. 1989), and observed with a Zeiss epifluorescence microscope.

Northern blot analysis

RNA was isolated using a TRI reagent RNA isolation kit (Molecular Research Center, Cincinnati, Ohio) following the protocol provided by the manufacturer. Briefly, 2×10^8 sporulated oocysts (Iowa isolate, AIDS Research and Reference Reagent Program) were homogenized in 1 ml TRI reagent with a polytron

homogenizer. After the addition of bromochloropropane and centrifugation, the RNAs in aqueous phase were precipitated by 70% ethanol and air-dried before dissolving in 20 µl of H_2O. RNA was stored at −70 °C before use. Northern blotting was performed as described by Novy et al. (1991). Approximately 5 µg of RNA sample were loaded on a 1% formaldehyde/agarose gel. After electrophoresis, the RNA was transferred to membrane. A 600-bp cDNA probe from SC1 was labeled with the Random primed DNA labeling kit. Hybridization and wash conditions were the same as described above, with the exception of a 60 °C wash instead of 37 °C.

Primer extension

The CP2 antisense primers Cpext1 (5′-GTGAGGATATGGTGAGGGAGCC-3′) corresponding to nucleotides (nt) 93–114, and Cpext2 (5′-GGGAGAAAATAGAAAAACACGGAGAG-3′) corresponding to nt positions −23 to +2 were used for primer extension experiments to determine the transcription initiation start site. Primers (1 µg/reaction) were labeled using T4 DNA polynucleotide kinase (Promega, Madison, Wis.) in the presence of γ-^{32}P-ATP (200 μCi/reaction; NEN, Boston, Mass.). Labeled primers (2×10^5 cpm) were incubated with 10 µg of total RNA, prepared from sporulated oocysts at 50 °C for 90 min. The extension reaction was performed at 42 °C for 1 h using M-MLV reverse transcriptase (Invitrogen, Carlsbad, Calif.). The reaction was stopped by phenol/chloroform extraction and the reaction products were precipitated with ethanol. Pellets were resuspended in 5 µl of formamide sequencing buffer and samples were loaded onto a 6% denaturing polyacrylamide gel. A sequencing reaction of a known gene was loaded on the gel along with the primer extension products to serve as a size marker.

3′ Rapid amplification of cDNA ends

3′RACE cloning was used to clone the 3′ region of CP2. First- and second-strand synthesis and subsequent RACE-PCR were carried out using the Marathon cDNA amplification kit (Clontech, Palo Alto, Calif.). Briefly, 2 µg of RNA were used for first-strand cDNA synthesis with 10 μM Marathon cDNA synthesis primer (5′-TTCTAGAATTCAGCGGCCGC$(T)_{30}$NN-3′) immediately followed by second-strand synthesis and adaptor ligation. After an initial denaturation step (94 °C for 1 min), PCR reactions were cycled 30 times at 94 °C for 5 s and 68 °C for 4 min with the adaptor primer (AP1, 5′-CCATCCTAATACGACTCACTATAGGGC-3′) and a *cp2* gene-specific primer, SC2RC (5′-CATCCGACAAGAATGAAGCCAATGATGCT-3′). The amplified PCR fragments with a size about 1.4 kb was gel-purified using the QIAEX II gel extraction kit (Qiagen, Chatsworth, Calif.) and subcloned into the TA vector (Invitrogen, Carlsbad, Calif.). Inserts from three independent clones were sequenced.

Results

Cloning and characterization of the *cp2* gene

A *C. parvum* cDNA clone, referred to as SC1, was initially obtained from a screen of a sporulated oocyst cDNA expression library, using antiserum CMYL30 (Yu et al. 2002) against *C. muris*. Using this clone as a probe for further cDNA screening of the library revealed that SC1 represented an abundant clone. Among many positive clones, several were plaque-purified and their inserts were subcloned into a pBluescript SK(+/−) vector for further characterization. Four representative clones (SC2, SC11, SC24, SC25) and the SC1 probe are shown in Fig. 1A. Nucleotide sequences of inserts from

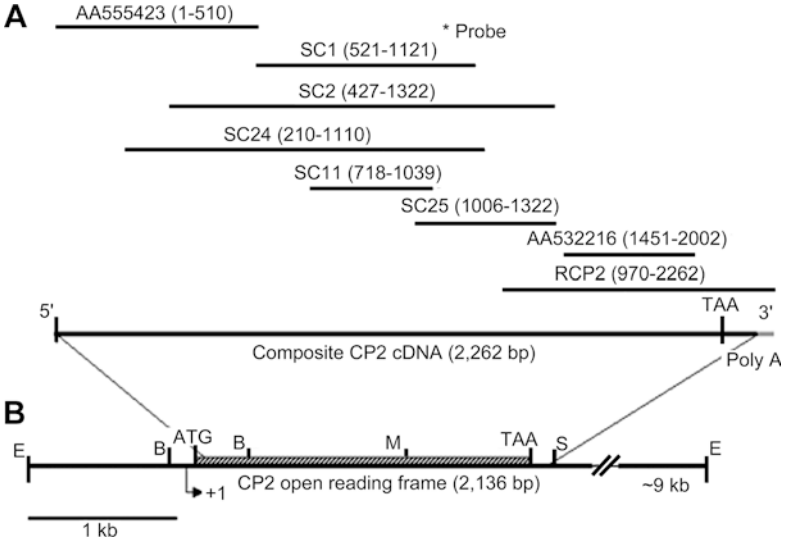

Fig. 1A, B Schematic diagrams of *cp2* cDNA and genomic clones. **A** Independent, overlapping *cp2* cDNA clones. Five independent clones (SC1, SC2, SC24, SC11, SC25) obtained from the screen of a sporulated oocyst cDNA library are diagrammed here in their relative positions. Together, all cDNAs resulted in a 1,112-bp composite sequence. A search of a *Cryptosporidium parvum* expressed sequence tag (EST) database revealed a 510-bp sequence of EST AA555423, which extended the 5′ region of the composite cDNA 210 bp. 3′RACE was performed to obtain the 3′ region of the *cp2* message (RCP2) and, together, a 2,262-bp *cp2* cDNA composite sequence was obtained. **B** A restriction enzyme map of *cp2* genomic clones. Five genomic clones, each approximately 9 kb, were obtained from a *C. parvum* genomic library, using SC1 as a probe. Regions of each genomic clone were sequenced (*bold line*) and all were identical. The *cp2* composite cDNA sequence and genomic sequence revealed an open reading frame (ORF) of 2,136 bp (*shaded box*) coding for a protein of 711 amino acid residues with a 3′ noncoding sequence of 140 bp. The transcription start site, as determined by primer extension, was noted. A second EST clone (AA532216) with sequence identical to the 3′ region of *cp2* genomic sequence further confirmed the CP2 ORF. *E Eco*R1, *B Bgl*II, *M Mfe*I, *S Sac*II

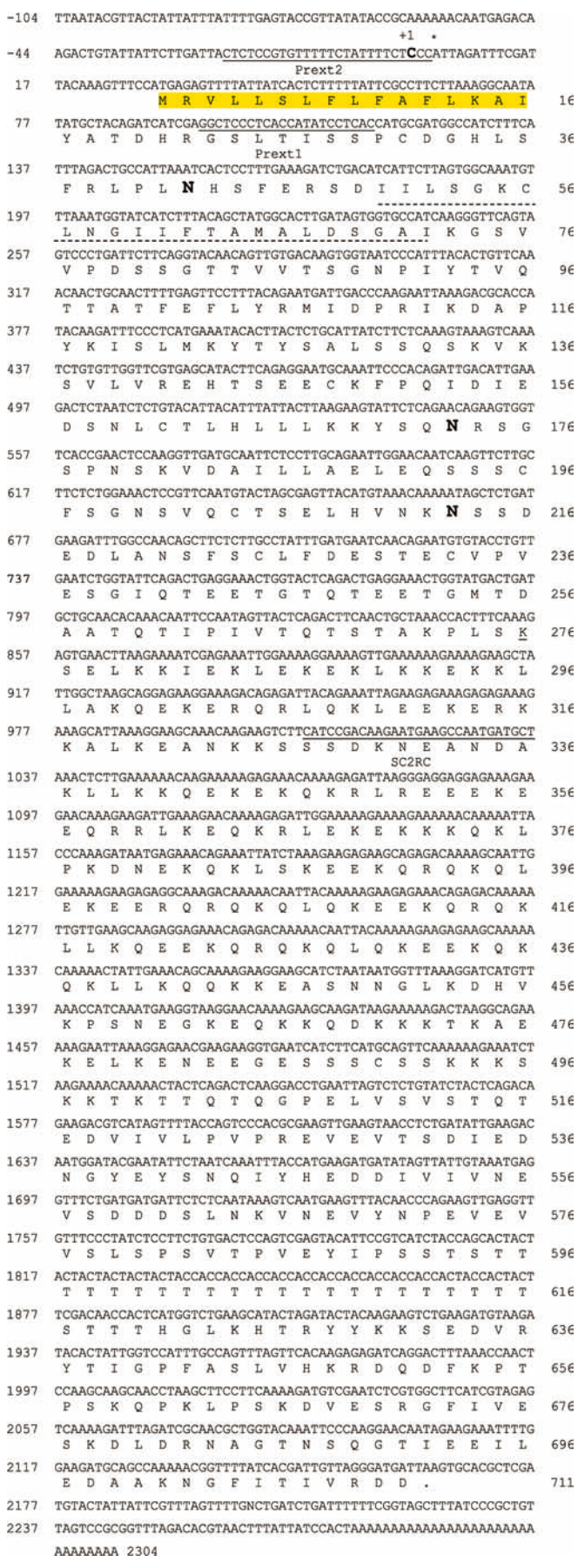

Fig. 2 Complete nucleotide sequence (*upper lines and numbers*) and deduced amino acid (aa) sequence (*one-letter code, lower lines and numbers*) of the *cp2* gene. The transcription start site is *in bold* (alternate transcription start site as seen by the doublet banding in primer extension reaction is *denoted by asterisks*). The position of the antisense primers Prext1 and Prext2, used in the primer extension reaction, are *underlined*, as is the sense primer, SC2RC, which was used for the 3′RACE reaction. The *cp2* message contains on ORF of 2,136 nucleotides (nt) with 28 nt of the 5′ noncoding region and 140 nt of the 3′ noncoding region. The signal peptide consensus sequence (aa 1–16) is highlighted and the putative transmembrane domain (aa 50–72) is underlined with a dashed line. Possible *N*-glycosylation sites (*N*) are shown *in bold and enlarged*

these clones revealed a total cDNA of 1,112 bp. The 5′ region of SC24 was used to search a *C. parvum* EST database (http://www.ncbi.nlm.nih.gov/BLAST/) and a 510-bp clone (accession number AA555423) extended the 5′ region 210 bp. A 3′RACE reaction, using total sporulated oocyst RNA and the primer SC2RC (nt 1,008–1,036; Fig. 2), was used to clone the 3′ region of the message (RCP2, Fig. 1A). Sequencing of RCP2 revealed a polyA addition site and a polyA tail. Thus, the composite CP2 cDNA obtained has a total of 2,262 bp (Fig. 1A). A *C. parvum* genomic library was also screened using SC1 as a probe; and five genomic

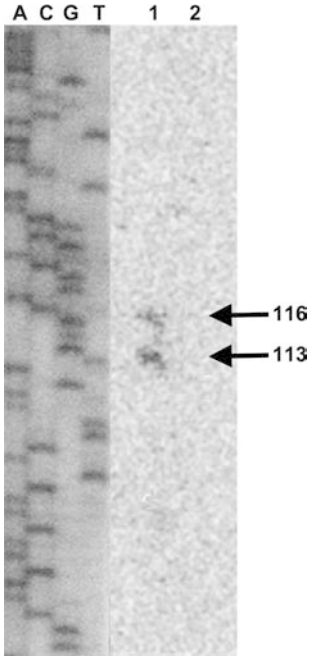

Fig. 3 Primer extension reaction mapping the transcription start site for *cp2* message. Doublet primer extension bands with 116 nt and 113 nt were detected using primer Prext1 (nt 116 5′-GTGAGGATATGGTGAGGGAGCC-3′ nt 95; *lane 1*). No product resulted using primer Prext2 (nt +3 5′-GGGAGAAAAT-AGAAAAACACGGAGAG-3′ nt −24; *lane 2*). These results, together with a consensus Kozak sequence for the start codon found in the composite *cp2* cDNA, suggest that the *cp2* message contains 25 nt or 28 nt of 5′ noncoding sequence. The *A, C, G, T lanes* contain the DNA sequence reaction of a known *C. parvum* genomic DNA clone

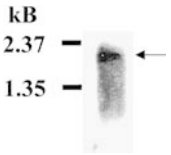

Fig. 4 Northern blot analysis of total RNA prepared from sporulated oocysts with a ^{32}P-labeled SC1 cDNA probe. A RNA band of approximate 2.3 kb was detected, which represents the *cp2* message size

clones, each with an insert approximately 9 kb in length, were obtained. Regions of the five genomic clones were sequenced and found to be identical. The largest open reading frame (ORF), based on genomic and composite CP2 sequence information, predicts a coding region of 2,136 bp with a 3′ non-coding region, including the polyA tail, of 140 bp. Figure 1B shows a restriction enzyme map of the CP2 genomic clone and the relative positions of the composite CP2 cDNA clones. A second EST, AA532216, was found to correspond to the 3′ region of the ORF, further confirming this conclusion. The nucleotide sequence for composite CP2 cDNA and its 5′ upstream sequence derived from a CP2 genomic clone are shown in Fig. 2. The deduced amino acid (aa) sequence for CP2 is also listed in Fig. 2, with a potential signal peptide indicated. Lysine and glutamic acid make up approximately 25% of the total protein and 50% of the aa sequence in the middle third of the protein, which has a predicted alpha helical or coiled-coil secondary structure. A search of an aa sequence database (FASTA) revealed similarities to various proteins, most of which fell into three distinct categories: cytoskeletal proteins including trichohyalin and caldesmon, *Plasmodium* antigens exported to the erythrocyte plasma membrane, and *Plasmodium* antigens belonging to the erythrocyte-binding protein family. Homologies were not extensive and most showed greatest similarity to the lysine/glutamic acid-rich region. The N-terminus of the peptide is a predicted signal peptide (aa 1–16); and numerous predicted sites for N-glycosylation (aa 42, 173, 213) and phosphorylation and a putative transmembrane domain (aa 50–72) are also present.

In an effort to determine the transcription start site, a primer extension reaction was performed. When total oocyst RNA was incubated with an antisense primer (Prext1, nt 95–116; Fig. 2), specific to the 5′ region (nt 58–79) of the 2,262-bp composite sequence, extended with reverse transcriptase, and analyzed on a denaturing polyacrylamide gel, bands of 116 bp and 113 bp were detected (Fig. 3). The products map 25 bp and 28 bp upstream from the designated start codon and represent the 5′ end of the *cp2* mRNA. In contrast, no product was observed when a second antisense primer (Prext2, nt −24 to +3), corresponding to genomic sequence data from a region further upstream (Fig. 2), was used. The

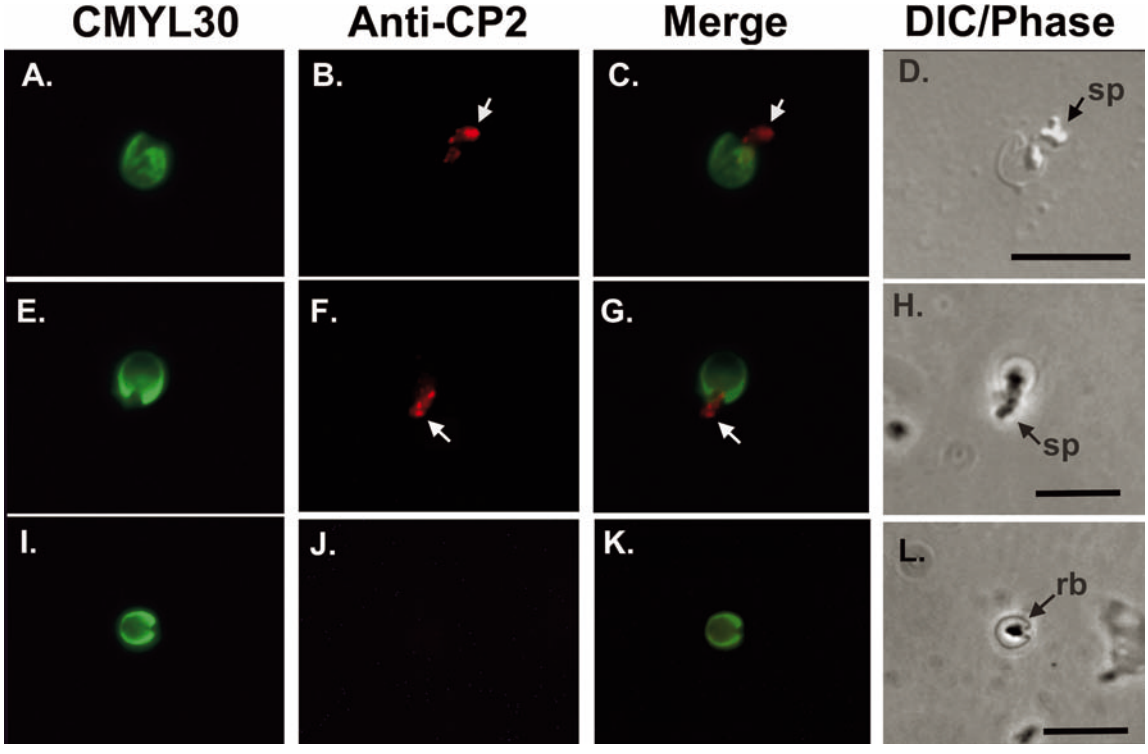

Fig. 5A–L Double-label immunofluorescence microscopy of excysted oocysts. Oocysts were allowed to excyst on Superfrost slides for 30 min prior to fixation and permeabilization. **A, E, I** Green fluorescence reveals the oocyst wall as recognized by the monoclonal antibody CMYL30 (Yu et al. 2002). **B, F, J** Red fluorescence image of the same fields as **A, E, I**, respectively, revealed by anti-CP2 polyclonal antibody. Anti-CP2 antibody reacts with the sporozoite (*sp*; *arrows* in **B, C, F, G**), but not the oocyst wall. No reactivity was observed in the residual body (*rb*; **J**). **C, G K** Merged images, respectively, of **A** and **B**, **E** and **F**, and **I** and **J**. **D, H, L** Phase images of the organisms. *Bar* 10 μm

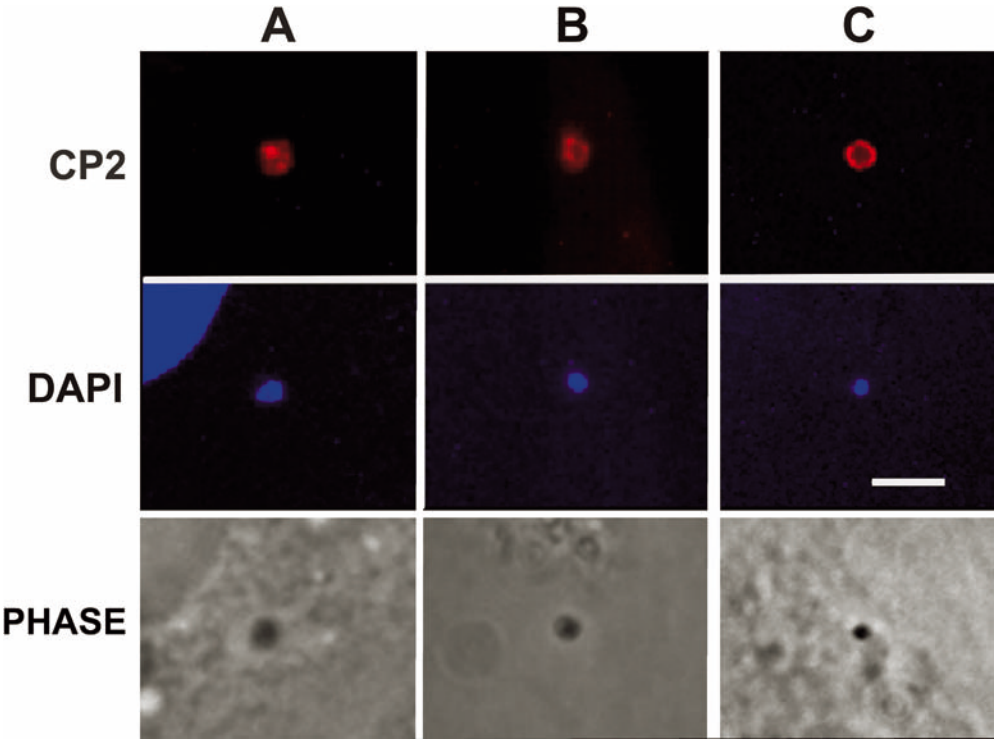

Fig. 6A–C Immunofluorescence microscopy of *C. parvum*-infected HCT-8 cells with anti-CP2 antibody (*CP2*) and 4′,6-diamidino-2-phenylindole (*DAPI*). Early infections exhibit staining as diffuse puncta (column **A**), or a ring-like distribution around the nucleus (columns **B, C**). Sporulated oocysts were added to cell culture and allowed to infect for 5–15 h. *Bar* 5 μm

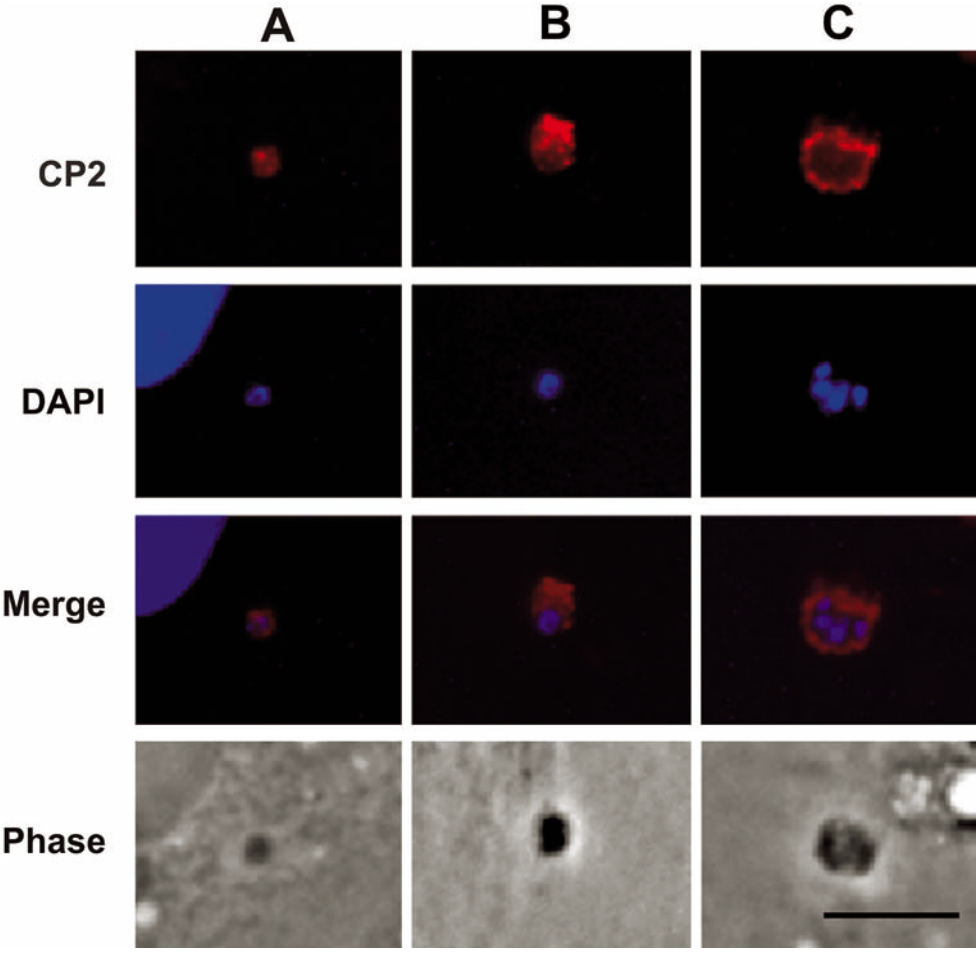

Fig. 7A–C Immunofluorescence of HCT-8 cells infected with *C. parvum* oocysts for 15 h. Infection sites were observed with indirect immunofluorescence using the anti-CP2 antibody and confirmed with DAPI staining and phase contrast microscopy. Columns **A** and **B** reveal infection sites with only one discernable nucleus as observed with DAPI staining. Column **C** reveals a more advanced meront with the CP2 antigen surrounding the parasite. *Bar* 10 μm

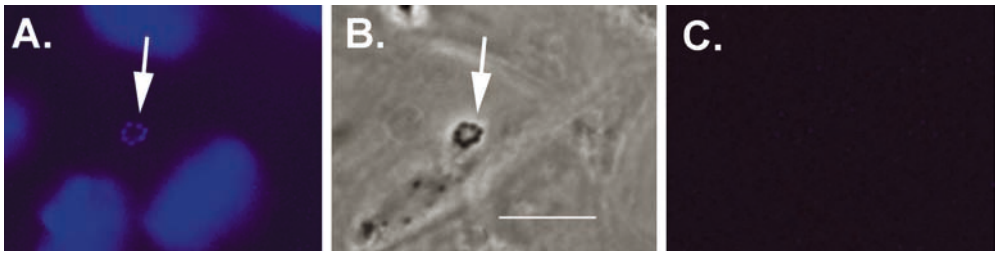

Fig. 8A–C Immunofluorescence microscopy of *C. parvum*-infected HCT-8 cells with pre-immune serum and DAPI nuclear stain. **A** DAPI stain reveals the presence of a meront. **B** Phase image of **A** and **C**. **C** Pre-immune serum does not react with the infection site

lack of product for this reaction (Fig. 3, lane 2) supports the localization of the transcription start site to the region defined by primer extension with the Prext1 primer. This result also indicates that the composite *cp2* cDNA sequence was lacking the first 37 nt at the 5′ end, resulting in a complete *cp2* message of 2,304 nt, with a 5′ noncoding region of 28 nt, a coding region of 2,136 nt and a 3′-noncoding region of 140 nt. When a total *C. parvum* RNA blot was probed with ^{32}P-labeled SC1, a major transcript of approximately 2.3 kb was detected (Fig. 4), which correlates well with the sequence information.

Localization of *cp2* gene product

CP2 localizes to sporozoites

Immunofluorescence microscopy was utilized to localize CP2 in oocysts, sporozoites, and in developing and mature type I meronts. Initially, oocysts were excysted and processed for immunofluorescence with the anti-CP2 antibody and the monoclonal antibody CMYL30 (Fig. 5A, E, I) against CM250 oocyst wall antigen (Yu et al. 2002). Anti-CP2 did not react with the oocyst walls, possibly due to the bleach treatment of oocysts, but fluorescence was observed on sporozoites (arrows in Fig. 5B, C, F, G). Figure 5J shows that the residual body of an empty oocyst is negative for the anti-CP2 antibody.

CP2 localizes to infection sites

The CP2 expression during early infection (5–15 h) was examined on human ileocecal cell line HCT-8. Single nuclei infection sites appeared at 5 h post-inoculation and were classified as trophozoites. Very few multinucleate infection sites were observed at this time point. Subsequent observations through 15 h post-inoculation revealed the formation of multinucleate structures which were considered type I meronts if 6–8 nuclei were observed. Infection sites at the single nucleus stage (trophozoite) revealed varied fluorescent patterns: some were less strictly organized (Fig. 6A) whereas many revealed a ring-like distribution (Fig. 6B, C). As the trophozoites matured and began the process of merogeny, the immunofluorescent signal increased in intensity and appeared to surround the mature type I meronts (Fig. 7C). Hence, there appears to be an abundance of CP2 gene product associated with the infection process and development of the asexual stage. Immunofluorescence using pre-immune serum was performed as a control (Fig. 8). The serum failed to recognize infection sites. The in vivo localization of CP2 was initially addressed by immunohistochemical staining of infected mouse ileum. Several infection sites were observed. The localization of CP2 at infection sites was similar to that found in infected HCT-8 cells, in that the antigen appeared to localize to the membranous structure surrounding the parasite (Fig. 9C, arrow). No staining was observed in the uninfected control section (Fig. 9A) or in infected tissue without anti-CP2 antibody (Fig. 9B).

Fig. 9 Paraffin-embedded, sectioned, uninfected (**A**) and infected ileum (**B**, **C**). Three-week-old female mice were infected with 1×10^7 oocysts. Mice were sacrificed 2 weeks post-infection and the distal ileum was removed and fixed in 3.7% formaldehyde prior to histochemical processing. **A** No staining was observed in the uninfected control sections. **B** No staining was observed in infected tissue without anti-CP2 antibody. **C** The anti-CP2 antibody recognized *C. parvum* infection sites on the lumenal surface of enterocytes. *Bar* 10 μm

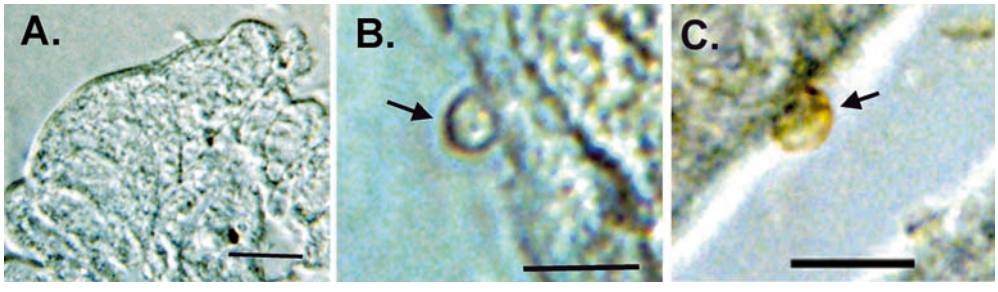

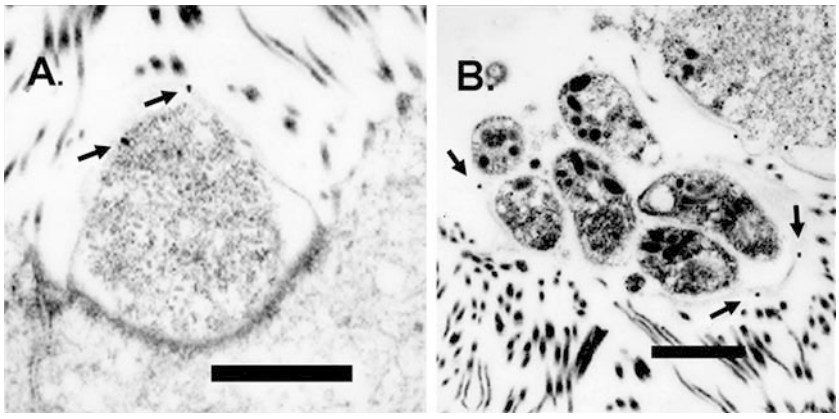

Fig. 10A, B Immunoelectron micrographs of asexual developmental stages of *C. parvum* using the polyclonal antibody anti-CP2. **A** Section through an early trophozoite stage parasite. A few reactive gold particles are seen at the parasitophorous vacuole membrane (PVM) and subjacent to this membrane (*arrows*). No reactive particles are seen at the parasite–host interface. **B** Section through a mature type I meront. A few reactive granules can be detected along the PVM, while no reactive gold particles are observed on or within the merozoites. *Bars* 1 μm

CP2 is localized on the PVM and other membranous structures

In order to further localize CP2 throughout the parasite life cycle, immunogold electron microscopy was utilized. Three-week-old mice were infected and mouse ileum was processed for electron microscopy. Figure 10A reveals minimal reactivity to an early trophozoite. Few gold particles associate with the PVM region or immediately beneath this membranous structure (Fig. 10A, arrows). A mature type I meront is shown in Fig. 10B. Again, few gold particles associate with the PVM in regions where the membrane is visible (arrows). Surprisingly, no gold particles were observed in the merozoites. Figure 11A–D illustrates the progression from an early macrogametocyte to a sporulated oocyst. Initially, gold particles are found in the amylopectin-like granules of an early macrogametocyte (Fig. 11A). Figure 11B shows that most electron-dense wall-forming bodies (arrowheads) are negative. Instead, the gold particles heavily decorate the periphery of amylopectin-like vesicles (arrows) and the cytoplasm proximal to these vesicles. An immature oocyst is shown in Fig. 11C. Again, the periphery of amylopectin-like granules and cytoplasm are labeled. Of note in this image is the localization of gold particle clusters at the periphery of the parasite subjacent to the parasitophorous vacuole (arrows) and between the parasite pellicle and PVM (arrowheads). An infection site harboring a fully sporulated oocyst is shown in Fig. 11D. Gold particles decorate the PVM and sporozoite membrane and the oocyst wall (Fig. 11E). Thus, CP2 was found, to some degree, on the PVM of all developmental stages examined.

Quantification of CP2 distribution throughout oocyst formation

In an effort to determine the distribution of CP2 throughout oocyst formation, a quantitative analysis of gold particle distribution from early macrogametocyte to sporulated oocyst was performed. The total number of gold particles was counted for each developmental stage (Table 1). The percentage of total particles at each structure listed was determined. Reactivity to the host cell was considered as the background level. The average percentage of gold particles localizing to the host cell was $3.4 \pm 2.1\%$. In the early macrogametocyte, the majority of gold particles were found in the amylopectin-like granules (53.8%) and cytoplasm (30.8%). The late macrogametocyte revealed the majority of gold particles in the parasite cytoplasm (83.7%). As the parasite progressed to the immature oocyst stage, the gold particles were again found in the amylopectin-like granules (36.3%) and parasite cytoplasm (31.3%). However, at this stage, we began to see a greater number of particles on or near the PVM or associated with the oocyst wall (12.4%). At the sporulated oocyst stage, most gold particles were associated with the PVM (17.5%), the oocyst wall (35.7%), or the sporozoite (35.7%). We therefore suggest a progression from amylopectin-like granules and cytoplasm towards membranous structures of the sporulated oocyst, including the oocyst wall, PVM, and sporozoite.

Discussion

In the present study, we cloned a novel *C. parvum* gene, *cp2*. The CP2 protein contains a putative signal sequence (aa 1–16) and a single hydrophobic domain (aa 50–72), suggesting that CP2 is a secreted/transmembrane protein. Amino acid residues in the middle third of the protein are rich in lysine and glutamic acid and have a predicted alpha-helical or coiled-coil secondary structure. Within this segment, there are five 10-aa repeating units (aa 387–441) within which is the consensus sequence (K/q)EE(K/r)Q(R/k)QK(Q/l)L.

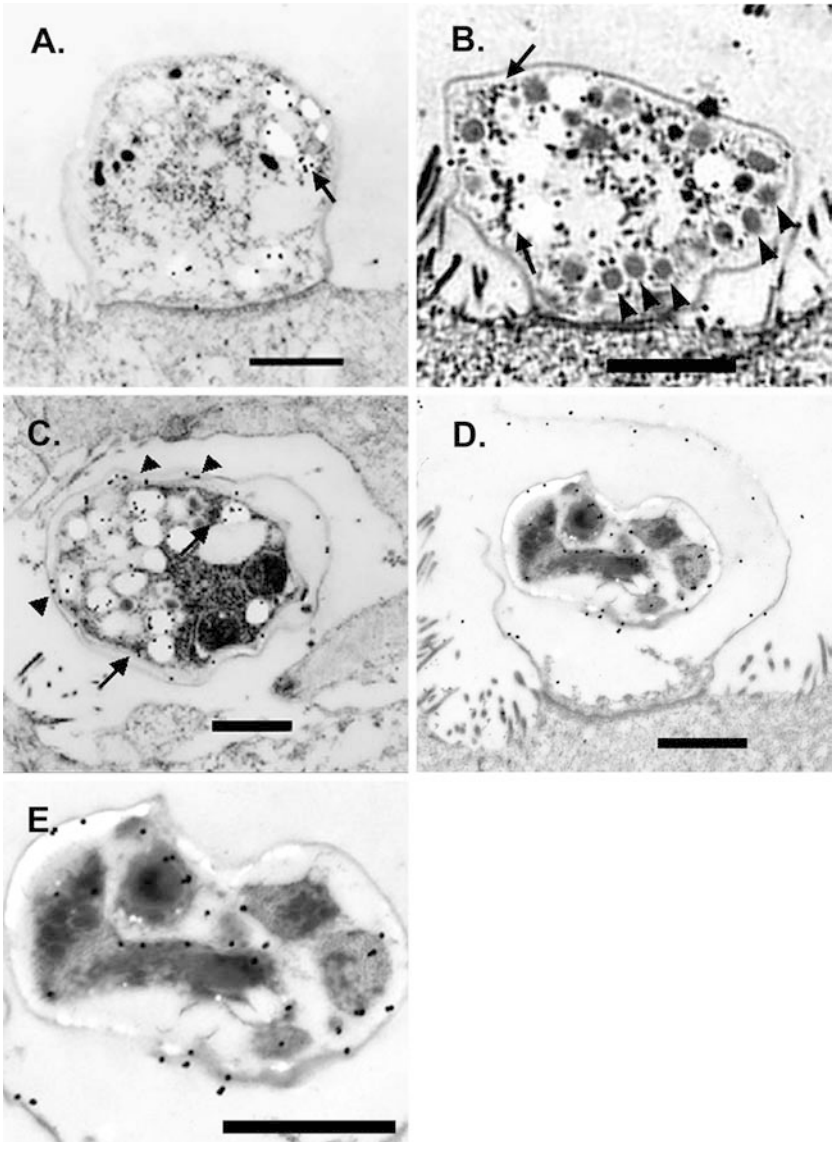

Fig. 11A–E Immunoelectron micrographs of the progression from a macrogametocyte to a sporulated oocyst, using the polyclonal antibody anti-CP2. **A** Thin section of an early macrogametocyte. Reactive gold particles are observed within the amylopectin-like granules (*arrows*). **B** A more advanced macrogametocyte with reactive gold particles adjacent to the amylopectin-like granules (*arrows*) and decorating some presumptive wall-forming bodies, while most are unlabeled (*arrowheads*). **C** An immature oocyst with labeling of the periphery of amylopectin-like granules. In addition, gold particle clusters are observed near the PVM (*arrowheads*) and in the vacuolar space (*arrows*). **D** Section through an infection site harboring a sporulated oocyst. Immunoreactive gold particles are observed along the PVM, the sporozoite membrane, and the oocyst wall. **E** Magnification of panel **cD** revealing gold particle decoration of the oocyst wall and sporozoites. *Bars* 1 μm

Immunofluorescence microscopy revealed a reactivity to sporozoites and none associated with the oocyst wall. The CP2 antigen was also detected early in the infection process in the trophozoite. The pattern of fluorescence changed throughout development from trophozoite to mature type I meront. Initially, the fluorescence pattern exhibited either a small ring-like structure or a diffuse pattern and progressed to a definitive ring-like structure seeming to encase the type I meront and associate with either the host-derived membrane or parasite pellicle. The temporal and spatial pattern of CP2 expression as determined by immunofluorescence suggest it may be integrally involved in the infection process.

Table 1 Quantification of immunogold labeling throughout oocyst formation, using anti-CP2 antibody. Data presented are percentage gold particles per specified structure. *N.A.* Not applicable, *PVM* parasitophorous vacuole membrane

Developmental stage	Structural feature of parasite							Host
	Amylopectin-like granules	Cytoplasm	PVM	Wall-forming bodies	Oocyst wall	Sporozoite	Feeder organelle membrane	
Early macrogametocyte	53.8	30.8	7.7	N.A.	N.A.	N.A.	2.6	5.1
Late Macrogametocyte	3.4	83.7	5.8	4.7	N.A.	N.A.	0	0.6
Immature oocyst	36.3	31.3	7.0	N.A.	12.4	N.A.	0	3.0
Oocyst	N.A.	8.7	17.5	N.A.	35.7	35.7	0	4.8

While immunofluorescence analysis in cultured cells was limited to asexual stages of development, immunogold electron microscopy revealed the antigen in several stages of the parasite life cycle. During asexual development (trophozoite, meront) CP2 can be seen, in small quantities yet consistently, on or near the PVM. Bonnin et al. (1995) describe dense granule antigens, recognized by monoclonal antibodies L01 and BKE, which localize to the PVM. Interestingly, these antigens remained present in Triton X detergent-extracted host cells, suggesting an interaction with the host (detergent-insoluble) cytoskeleton. The fluorescent pattern observed was similar to CP2. Both monoclonal antibodies L01 and BKE reacted with a carbohydrate moiety. In fact, most *C. parvum* antigens localized to the PVM using immunological microscopic techniques reacted with carbohydrate epitopes that were present as multiple bands in Western blot analysis (Ward and Cevallos 1998). Here, we show the expression pattern of CP2, a peptide recognized by polyclonal antibodies that is expressed in several stages of development and localizes to membranous structures of all stages characterized.

It is not clear how CP2 is transported to or what function it serves on the PVM. In the macrogametocyte, two distinct oocyst wall-forming bodies have been described in which components of the wall are possibly exocytosed between the limiting membranes of the macrogametocyte (Current and Reese 1986). Bonnin et al. (1991) suggested oocyst wall antigens of *C. parvum*, recognized by monoclonal antibody OW IG0, are released into the vacuolar space from distinct, electronlucent vesicles and are subsequently incorporated into the oocyst wall. In this study, we showed that the transfer of CP2 to the host-derived PVM may occur from distinct vesicles, first to the vacuolar space, and finally to the PVM. We also observed gold particle decoration of the oocyst wall but not with immunofluorescence, suggesting bleach treatment of oocysts may alter the reactive epitope. Thus, a similar mechanism of exocytosis may exist for the transport of CP2 during parasite development. The transfer of parasite molecules to the host-derived PVM of the other life-cycle stages must occur through a different mechanism. One obvious mechanism is the release of molecules from apical organelles or the membrane during the invasion process, as has been observed in other apicomplexans (Beckers et al. 1994; Carruthers and Sibley 1997; Saffer et al. 1992; Sinai and Joiner 2001). While localization of CP2 in sporulated oocysts suggests reactivity to the sporozoite surface, it may be worthwhile to further characterize the distribution in invasive sporozoites.

The function of *Cryptosporidium* molecules in the PVM is not known, but evidence suggests membrane modifications at the level of the parasite plasma membrane in other apicomplexan species. It is proposed that modifications in these species may play a role in the transportation or secretion of molecules to and from the parasite (Dubremetz and Schwartzman 1993). Host membrane modifications in *Plasmodium*-infected erythrocytes have also been described (Grellier et al. 1991; Pouvelle et al. 1991). Protein targeting beyond the parasite plasma membrane in *P. falciparum* is thought to be achieved through several membranous structures of parasite origin. Modifications to the infected erythrocyte membrane serve as a mechanism to increase the adhesive properties of erythrocytes to keep them from being cleared by the spleen, aid in the transport of molecules to and from serum, or serve as a protective, variable antigen on the surface of infected cells. One could envision that CP2 in the PVM may be involved in some aspect of membrane integrity, either stabilizing or acting as a mechanism to breakdown those structures through interactions with the host membrane and/or cytoskeleton. Alternately, CP2 may be involved in some aspect of molecular transport to or from the enteric lumen.

Acknowledgements We would like to thank Dr. George Cain for critical reading of the manuscript. This work was supported by grant HD18577 from the National Institutes of Health (J.J.C.L.) and grant 2000-1-20200-003-1 from the Basic Research Program of Korean Science and Engineering Foundation (J.R.Y.). The following reagents were obtained through the AIDS Research and Reference Reagent Program, Division of AIDS, NIAID, the National Institutes of Health: *C. parvum* oocysts provided by Ms. Marilyn Marshall and Dr. Charles Sterling, *C. parvum* cDNA and genomic libraries produced by BioTechnology General. The experiments comply with the current laws of the United States in which the experiments were performed. The nucleotide sequence reported in this paper has been submitted to the GenBank with accession number AY471868.

References

Beckers CJM, Dubremetz JF, Mercereaupuijalon O, Joiner KA (1994) The *Toxoplasma gondii* rhoptry protein Rop-2 is inserted into the parasitophorous vacuole membrane, surrounding the intracellular parasite, and is exposed to the host cell cytoplasm. J Cell Biol 127:947–961

Bonnin A, Dubremetz JF, Camerlynck P (1991) Characterization and immunolocalization of an oocyst wall antigen of *Cryptosporidium parvum* (Protozoa, Apicomplexa). Parasitology 103:171–177

Bonnin A, Gut J, Dubremetz JF, Nelson RG, Camerlynck P (1995) Monoclonal antibodies identify a subset of dense granules in *Cryptosporidium parvum* zoites and gamonts. J Eukaryot Microbiol 42:395–401

Carruthers VB, Sibley LD (1997) Sequential protein secretion from three distinct organelles of *Toxoplasma gondii* accompanies invasion of human fibroblasts. Eur J Cell Biol 73:114–123

Casemore DP, Armstrong M, Sands RL (1985) Laboratory diagnosis of cryptosporidiosis. J Clin Pathol 38:1337–1341

Current WL, Reese NC (1986) A comparison of endogenous development of 3 isolates of *Cryptosporidium* in suckling mice. J Protozool 33:98–108

Dubremetz JF, Schwartzman JD (1993) Subcellular organelles of *Toxoplasma gondii* and host cell invasion. Res Immunol 144: 31–33

Dubremetz JF, Garcia-Reguet N, Conseil V, Fourmaux MN (1998) Apical organelles and host cell invasion by Apicomplexa. Int J Parasitol 28:1007–1013

Grellier P, Rigomier D, Clavey V, Fruchart JC, Schrevel J (1991) Lipid traffic between high density lipoproteins and *Plasmodium falciparum* infected red blood cells. J Cell Biol 112:267–277

Hegmann TE, Lin JLC, Lin JJC (1989) Probing the role of non-muscle tropomyosin isoforms in intracellular granule movement by microinjection of monoclonal antibodies. J Cell Biol 109:1141–1152

Jin JP, Lin JJC (1989) Isolation and characterization of cDNA clones encoding embryonic and adult isoforms of rat cardiac troponin T. J Biol Chem 264:14471–14477

Lumb R, Smith K, Odonoghue PJ, Lanser JA (1988) Ultrastructure of the attachment of *Cryptosporidium* sporozoites to tissue culture cells. Parasitol Res 74:531–536

McDonald V, McCrossan MV, Petry F (1995) Localization of parasite antigens in *Cryptosporidium parvum* infected epithelial cells using monoclonal antibodies. Parasitology 110:259–268

Novy RE, Lin JLC, Lin JJC (1991) Characterization of cDNA clones encoding a human fibroblast caldesmon isoform and analysis of caldesmon expression in normal and transformed cells. J Biol Chem 266:16917–16924

Petry F, Robinson HA, McDonald V (1995) Murine infection model for maintenance and amplification of *Cryptosporidium parvum* oocysts. J Clin Microbiol 33:1922–1924

Pouvelle B, Spiegel R, Hsiao L, Howard RJ, Morris RL, Thomas AP, Taraschi TF (1991) Direct access to serum macromolecules by intraerythrocytic malaria parasites. Nature 353:73–75

Robert B, Antoine H, Dreze F, Coppe P, Collard A (1994) Characterization of a high molecular weight antigen of *Cryptosporidium parvum* micronemes possessing epitopes that are cross-reactive with all parasitic life cycle stages. Vet Res 25:384–398

Saffer LD, Mercereaupuijalon O, Dubremetz JF, Schwartzman JD (1992) Localization of a *Toxoplasma gondii* rhoptry protein by immunoelectron microscopy during and after host cell penetration. J Protozool 39:526–530

Sinai AP, Joiner KA (2001) The *Toxoplasma gondii* protein ROP2 mediates host organelle association with the parasitophorous vacuole membrane. J Cell Biol 154:95–108

Tzipori S, Griffiths JK (1998) Natural history and biology of *Cryptosporidium parvum*. In: Tzipori S (ed) Advances in parasitology: opportunistic protozoa in humans. Academic Press, San Diego, pp 5–36

Upton SJ, Tiley M, Brillhart DB (1995) Effects of select medium supplements on in vitro development of *Cryptosporidium parvum* in HCT-8 cells. J Clin Microbiol 33:371–375

Ward H, Cevallos AM (1998) *Cryptosporidium*: molecular basis of host–parasite interaction. In: Tzipori S (ed) Advances in parasitology: opportunistic protozoa in humans. Academic Press, San Diego, pp 151–185

Yu JR (1998) Distribution of actin and tropomyosin in *Cryptosporidium muris*. Korean J Parasitol 36:227–234

Yu JR, Chai JY (1995) Localization of actin and myosin in *Cryptosporidium parvum* using immunogold staining. Korean J Parasitol 33:155–164

Yu JR, O'Hara SP, Lin JLC, Dailey ME, Cain G, Lin JJC (2002) A common oocyst surface antigen of *Cryptosporidium* recognized by monoclonal antibodies. Parasitol Res 88:412–420